

**MODELING THE EFFECTS OF EPOXY DEBONDING ON
BONDED INSULATED RAIL JOINTS SUBJECTED TO
LONGITUDINAL LOADS**

Daniel C. Peltier

Graduate Research Assistant, Railroad Engineering Program
Department of Civil and Environmental Engineering
University of Illinois at Urbana-Champaign
B118 Newmark Civil Engineering Laboratory
1205 N. Mathews Ave.
University of Illinois at Urbana-Champaign
Urbana, IL 61801
Phone: (217)-244-6063
Fax: (217) 333-1924
Email: peltier2@uiuc.edu

Christopher P. L. Barkan

Associate Professor
Department of Civil and Environmental Engineering
University of Illinois at Urbana-Champaign
1201 Newmark Civil Engineering Laboratory
1205 N. Mathews Ave.
University of Illinois at Urbana-Champaign
Urbana, IL 61801
Phone: (217)-244-6338
Fax: (217) 333-1924
Email: cbarkan@uiuc.edu

ABSTRACT

Bonded (glued) insulated rail joints are widely used in continuously welded railroad track. These joints frequently develop problems in which the epoxy debonds from the fishing surfaces of the rail and joint bars, leading to problems such as pull-aparts and electrical failures. Insulated joint problems can be disruptive to railroad operations, and may in some cases increase the risk of train derailments.

This paper describes the results of computer modeling of the effects of epoxy debonding on the stresses and strains in a bonded insulated joint subjected to longitudinal force. The primary goal of this research is to identify measurable changes in the joint's strain distribution that correlate with the extent of debonding, to serve as the basis of a non-destructive monitoring and evaluation technique.

The results of the modeling show that, under thermal tensile loads, strains at the center of the outer surface of the joint bar tend to increase as debonding begins near the endpost. The strain at this point tends to stabilize after the debonding reaches the innermost bolt hole. Strain at a point between the outermost and middle bolt holes starts off relatively stable, but increases after debonding passes the innermost bolt hole. Strains in the event of a pull-apart depend on the friction parameters chosen for the ruptured epoxy. In all cases, results suggest that any increase in debonding causes an increase in the elastic relative displacement of the rail ends under load.

1. INTRODUCTION

Insulated rail joints (IJ's) are widely used throughout the North American rail network. Most mainline track uses “bonded” or “glued” IJ's (Figure 1), in which the insulator separating the joint bars from the rails is embedded in a strong epoxy. The epoxy binds the joint bars to the rails and allows very little relative movement. Although bonded IJ's have greater structural stiffness than unbonded ones (1), they still have shorter service lives than most other track components, especially on lines with dense traffic and high axle loads (2).



FIGURE 1: Typical Bonded Insulated Rail Joint

Epoxy debonding – the loss of electrochemical bond between the epoxy and metal surfaces – is a common precursor to IJ service failure. Davis et al. (2) identify a sequence

of events representing “the most typical failure scenario of bonded IJ’s in HAL service.” This sequence starts with part of the epoxy layer debonding from the rail, joint bar, or both. Debonding begins at the endpost and slowly extends outward towards the edges of the joint. The joint gets looser and looser, with increased vertical deflections, poorer load distribution, and larger relative motions between the components.

Further developments may include damage to the track substructure, water penetration and fretting, and electrical failure of the joint. Or, as the portion of the epoxy carrying shear stress decreases and shear strain within the epoxy increases, the shear load carried by the bolts increases; broken bolts or cracks in the joint bar or rail web can result. These latter problems may be preceded by a “pull-apart”, in which the rails permanently and visibly slip relative to the joint bars in response to high longitudinal rail forces. A pull-apart is taken to indicate that the epoxy has either debonded completely from the rail or ruptured along a surface parallel to the epoxy / rail interface.

Relatively new FRA regulations require visual inspections of IJ’s in continuous welded rail once or twice a year (3). While a visual inspection can detect advanced problems such as pull-aparts or broken bolts, and can detect some secondary evidence of looseness in the joint, most actual epoxy debonding is hidden from view in the interior of the joint. Debonding at the edges of the epoxy layer is visible, but these exterior edges may not give a complete picture of what is happening underneath the joint bar.

After a joint has been condemned and removed from the track, it is possible to pry off the joint bars and identify areas of epoxy debonding (Figure 2). These areas will typically show a brown discoloration due to rust. Areas that remained bonded will either

show a shiny surface (if the prying action separates the epoxy from the metal) or a rough epoxy-and-fiber fracture surface (if the prying action ruptures the epoxy layer).



FIGURE 2: Disassembled IJ. Rusty areas show where the epoxy debonded from the metal.

Visual inspections have another disadvantage: they are labor-intensive. This limits the frequency with which they can be conducted, which in turn limits the ability of maintenance forces to watch trends, predict failure, and schedule joint replacement accordingly.

We are researching ways to improve IJ condition monitoring. The goal is to develop a system based on leave-in-place sensors (strain gauges, extensometers, etc.) that can track changes in IJ properties over time and alert maintenance personnel when those changes indicate developing problems. In particular, this research has focused on the use of strain gauges and extensometers to measure and monitor the extent of epoxy debonding in a joint. The basis for this research is the assumption that changes in the

state of the epoxy bond will lead to changes in the strain distribution in the components of the IJ when the joint experiences thermal longitudinal loads.

This paper describes computer analysis using the finite element method that was performed in order to understand the effect of debonding on stresses and strains within a joint. Analysis results are currently being verified by an ongoing laboratory test program at the University of Illinois; preliminary laboratory results are discussed in this paper only to motivate the choice of certain model parameters.

The predicted behavior of IJ's under tensile longitudinal loads, the kinds that develop when the temperature drops below the rail neutral temperature, reveals some measurable changes in joint strain that are indicative of epoxy debonding. These changes in IJ behavior provide a potential method for indirectly but accurately measuring condition of the epoxy bond non-destructively.

2. PREVIOUS WORK

The behavior of rail joints subjected to wheel loads has been a subject of research since the early decades of the 20th century. The AREA-ASCE Special Committee on Stresses in Railroad track devoted large sections of its Fifth, Sixth, and Seventh Progress reports (1929, 1933, and 1940) to analyzing and measuring joint deflections and stresses (4). More recent work focuses on the dynamic loads caused by wheels passing over joints (5, 6). The widespread introduction of continuous welded rail (CWR) has reduced the importance of conventional rail joints, but has magnified the importance of insulated joints. This is partly because IJ's now represent a large percentage of all discontinuities in mainline track, and partly because, as axle loads have increased, other track components

have been strengthened in response. Consequently the problems caused by IJ's have become proportionally more important. In addition, CWR track tends to develop much higher longitudinal rail forces than jointed track, subjecting insulated joints to previously unknown stresses.

Arnold Kerr and Joel Cox at the University of Delaware studied the problem of insulated joints as a structural "weak spot" in the track (1). They developed an analytical model for deflection of a bonded IJ deflection under vertical loads, using three beams (two semi-infinite rail segments and one pair of joint bars) connected by vertical springs (7). This model does not distinguish between load transfer by compressive normal forces (the head of the rail pressing down on the top of the joint bar), tensile normal forces (the base of the rail pulling on the bottom of the joint bar), and shear forces (longitudinal bending stresses transferred from rail to bar through the epoxy bond). Since epoxy debonding prevents load transfer via epoxy shear or tension, but allows load transfer through epoxy compression, this analytical model does not appear conducive to studying the effects of debonding.

The Association of American Railroads Affiliated Laboratory at Virginia Polytechnic Institute and State University and the AAR's Transportation Technology Center, Inc. have used both computer modeling and field testing to compare the epoxy stresses of existing and experimental IJ designs with an intact epoxy bond (8, 9). The computer modeling of the conventional IJ design assumes one plane of symmetry and ignores the existence of bolt holes (10). Unlike Kerr's work, this numerical approach considers the combined effects of tensile (thermal) and vertical loadings, and predicts internal stresses within the joint.

This paper describes a similar approach, but with two important differences. The first is that the focus is not on the stresses and strains within the epoxy layer, but rather on the external surfaces of the joint. That is because the ultimate goal of this study is not to reduce stress and delay failure, but rather to measure stress and detect failure. The second difference is that, instead of comparing fully-bonded models of different joint designs, this paper compares the same joint design with differing degrees of epoxy debonding. Finally, this paper does not address vertical loads, as it is believed that the response of a joint to thermal tensile loads will be sufficient to determine the condition of the epoxy bond. Further work would be required to understand how debonding affects stresses under wheel loads.

3. FINITE ELEMENT MODEL

Two separate finite element models were created, representing bonded IJ's from two different suppliers. Both joints use an unworn 136RE rail section, identical material properties, and 36-inch (920 mm) joint bars with conventional bolt spacing. Only the shapes of the joints bars differed between the two models. Results described below apply equally to both models.

The model geometry was created with Pro ENGINEER Wildfire 3.0, exported to IGES files, and imported into MSC.Patran 2005. Patran was used to adjust the models, define material and section properties, impose load and boundary conditions, and mesh the model. The elements were then analyzed using ABAQUS 6.4; postprocessing was done using a combination of ABAQUS CAE and Patran.

3.1 Geometric Properties

Rail section geometries were obtained from the AREMA manual (11). Joint bar suppliers graciously provided joint bar dimensions and approximate epoxy layer widths.

Previous finite element analyses, which focused on stresses in the epoxy layer near the endpost, could safely ignore the presence of bolts or even bolt holes in the IJ (10). Our model, on the other hand, is designed to study strains over a much wider area, making the stress-rising effects of bolt holes quite important. The result is a relatively complicated geometry, consisting of boundary representation (B-rep) solids composed of curved faces with internal holes.

In a fully bonded joint, load is transferred from the rail to the joint bar via shear stresses in the epoxy, and the bolts do not play a significant structural role. However, with sufficient epoxy debonding, displacements may become large enough to deform the bolts, at which point load is transferred through shear in the bolts themselves. Thus the bolts also must be included in the model for their potential load-bearing function. The 1-inch (25.4 mm) bolts sit in a 1.25-inch (31.8 mm) hole, surrounded by a 3/32 inch (2.4 mm) layer of insulating material which is bonded to the bolt holes, leaving a 1/32 inch (0.8 mm) gap between bolt and insulator.

A fully-bonded IJ subject to pure longitudinal loads has two symmetry planes: one transverse vertical plane through the endpost, and one longitudinal vertical plane through the center of the railhead. However, there is no guarantee that any debonding will follow this symmetry. In order to retain flexibility to model any debonding pattern, the model does not exploit this symmetry.

3.2 Mesh Properties

The mesh used for the rails and joint bars used 10-node tetrahedral solid elements with material properties typical of carbon steel. The insulating epoxy layer consisted of a single layer of 10-node tetrahedra, with material properties based on standard industrial epoxies and technical advice from IJ researchers.

The epoxy and steel were connected using contact surfaces. For a fully bonded joint, these contact surfaces were “tied”, meaning nodes on both sides of the interface experience equal displacements. Debonding was modeled by dividing the contact surfaces into two parts: a tied section, representing an intact epoxy bond, and a “general contact” surface, which allows the two sets of nodes to slip tangentially or separate in the normal direction.

Limited destructive testing shows that debonding can occur between the rail and the epoxy layer, between the epoxy and the joint bar, or both. Modeling debonding only at the joint bar / epoxy interface can lead to some unrealistically large tensile stresses in the epoxy near the endpost. Brief experiments with the model showed that debonding on both surfaces did not cause significantly different results from debonding at the rail / epoxy interface only. Consequently, debonding was modeled at the rail / epoxy interface only.

Because the joint bars are pressed to the rails by the bolts, it is possible for frictional shear stresses to develop between debonded epoxy and the rail. Such friction will be concentrated in areas near the bolt holes, where normal stresses are highest, and therefore can be safely ignored for small amounts of debonding near the endpost. When the debonding is more extensive, the possible implications of this friction were explored,

using the ABAQUS stick / slip Coulomb friction model at the general contact surfaces. Because thermal longitudinal stresses in the rail tend to develop rather slowly, the coefficient of friction μ is modeled as a constant.

Contact surfaces were also used between the bolt and the bolt-hole insulators. Minimal additional constraints were imposed on the bolts to prevent rigid-body motion.

Three considerations determine the mesh size. First, the mesh on the epoxy surfaces must be fine enough to provide reasonable resolution in defining the debonded areas. Second, the mesh must be able to conform to the complicated model geometries, including the very thin epoxy layer and the irregular rail web, without producing unacceptably poor element geometries. Third, the number of nodes must be kept as small as possible to speed computation. For both joint models, about 150,000 nodes were required to meet the first two conditions using Patran's built-in meshing algorithms. Between 13,000 and 26,000 of these were fully constrained to other nodes via tied surfaces. To reduce computational complexity, the slave surface of the general contact pairs used to represent debonded interfaces included only 1/3 of the nodes available on that surface.

3.3 Loads and Boundary Conditions

A 40-kip (180 kN) tensile load was applied through the neutral axis of the rail on one end of the joint. This is approximately equal to the force that would result from a -20°F (-11°C) change in temperature. The other end was fixed in the longitudinal direction at a single point, also on the rail's neutral axis. Minimal additional constraints were imposed to prevent rigid-body motion only.

No other longitudinal restraints (such as rail anchors) were included. Because the bonded IJ allows only very small relative displacements between the two rail sections, it is expected that anchors will carry relatively little force compared to the tension that is transmitted through the joint bars themselves – at least on tangent track, under thermal loads only.

For cases involving debonding, a 50-kip (220 kN) confining force was applied at the edge of each bolt hole on the outside surface of the joint bar in a separate load step. This ensures that the state of the contact surface when the load is first applied represents the real-life situation, in which the bolts squeeze the bars onto the rails.

3.4 Computational Performance

The analysis was run on a 3 GHz Pentium 4 processor with 2 GB of memory. As might be expected, the time required to run the analysis depended greatly on the size of the nonlinear contact surfaces used to represent the areas of epoxy debonding. For a fully-bonded IJ, where contact between bolts and bolt holes can be ignored, a linear analysis required about 15 minutes of processing (excluding model verification). On the other extreme, a scenario representing a “pull-apart”, in which the entire epoxy surface had debonded, took over 7 hours to run. This situation is computationally expensive for three reasons:

- 1.) The large contact surfaces require many iterations to determine where the epoxy and metal interact and where they don't.

- 2.) Friction becomes relevant in this case, causing additional iterations as nodes experience stick-slip behavior.
- 3.) Friction causes hysteresis effects, with the displacements during the loading being lower than the displacements during unloading. In order to see these effects, the tension load must be applied in several increments, and then removed in several more increments.

Consistent with other assumptions made in the model, the loads were assumed to develop slowly, allowing the use of a static analysis for each load increment.

4. FINDINGS

4.1 Symmetric Debonding – No Friction

Figures 3-6 shows a progression representing the changes in deformation of an IJ under a 40-kip (180 kN) tension load as debonding spreads symmetrically outward from the endpost. Because of the symmetry, only one half of the joint bar is depicted. No frictional forces are included in these scenarios. There are four features worth noting:

- 1.) The strain in the joint bar near the endpost increases with increased debonding, up to a certain point.
- 2.) Strains in the joint bar farther away from the endpost increase only for larger amounts of debonding.
- 3.) The amount by which the gap between rails opens up under load increases with increased debonding.

FIGURE 3.a: Fully Bonded Joint

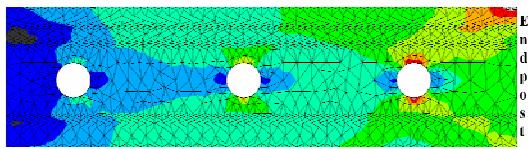


FIGURE 3.b: 1 Inch Debonding

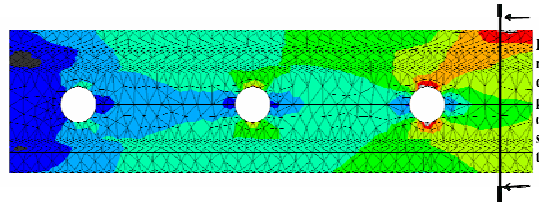


FIGURE 3.c: 2 Inch Debonding

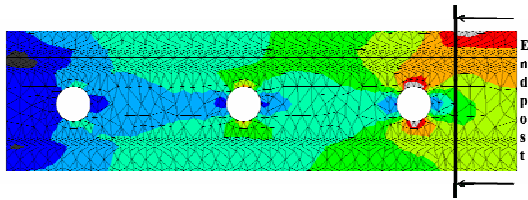


FIGURE 3.d: 3 Inch Debonding

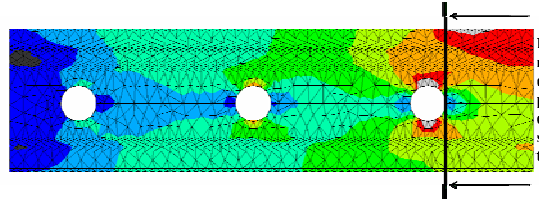


FIGURE 3.e: 6 Inch Debonding

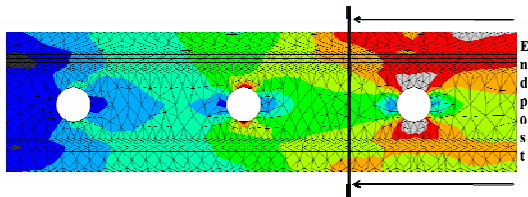
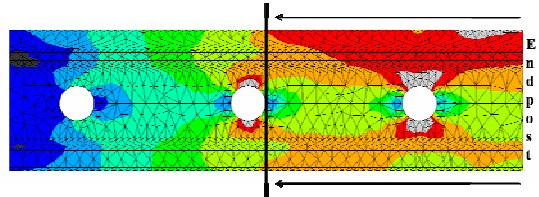


FIGURE 3.f: 9 Inch Debonding



Scale

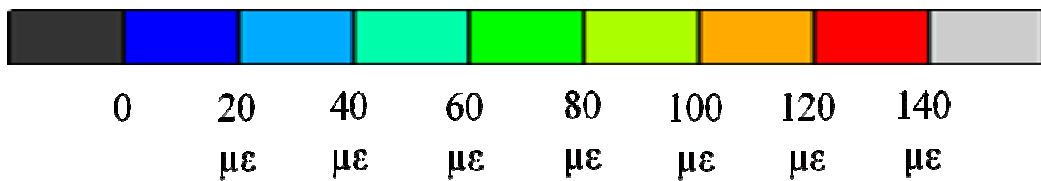


FIGURE 3: Longitudinal Strain in Joint Bar, 40k Tension

4.1.1 Strain Near Endpost

Tensile strain in the joint bar near the endpost becomes larger as debonding begins.

Simple static analysis says that the total tensile load carried by the joint bar at this

location is the same regardless of debonding, so the apparent increase must be caused by a change in how the tensile stress is distributed across the cross-section of the joint bar.

Figure 4 shows how the strain distribution through the joint bar cross-section at the center of the joint changes with debonding. While debonding does not affect the average tensile strain at the center of the joint bar, it does tend to increase the strain *at the outside surface of the bar*, where a strain gauge could feasibly be placed. When the epoxy transfers shear stress to the joint bar near the endpost, this shear shows up in the joint bar as an uneven longitudinal strain. As the epoxy debonds at this location, the shear strain in the joint bar diminishes and the longitudinal strain becomes more even.

When the debonded area extends past a certain point, the stress distribution will equalize laterally across the joint bar cross section and the strain on the outer surface will not increase with further debonding. Note that the strain on the outer surface of the joint bar changes very little between Figures 4.d and 4.f, compared with the change that occurs between figures 4.a and 4.c.

FIGURE 4.a: Fully Bonded Joint

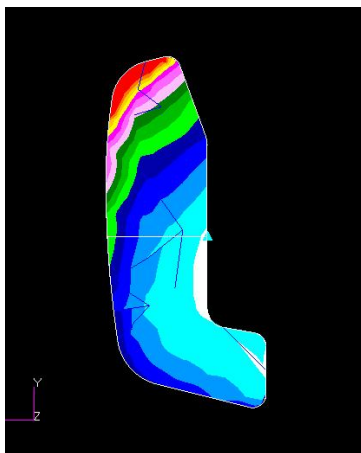


FIGURE 4.b: 0.5 Inch Debonding

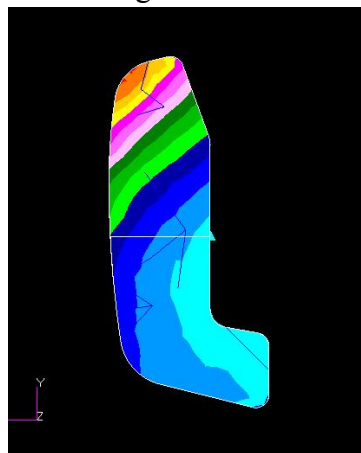
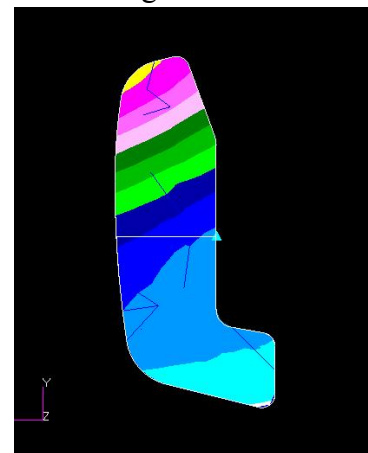


FIGURE 4.c: 1.25 Inch Debonding



to 230 mm) (Figures 3d through 3f). Strains near the outer edge of the joint bar begin to increase substantially only once debonding grows to cover the majority of the joint bar.

4.1.3 Longitudinal Relative Displacement of Rail Ends

Figure 5 shows the deformation of an IJ under the same load as before (magnified by a factor of 1000). The debonding is symmetric, extending by the indicated amount to either side of the endpost. Note that even in a fully-bonded joint the rail ends will move apart by a small amount when tension is applied. As debonding progresses, this relative motion of the rail ends gets larger and larger. This does not represent a “pull-apart”: the joint is not slipping permanently or visibly, but the elastic deformation is increasing in a way that could be measured using extensometers.

FIGURE 5.a: Fully Bonded Joint

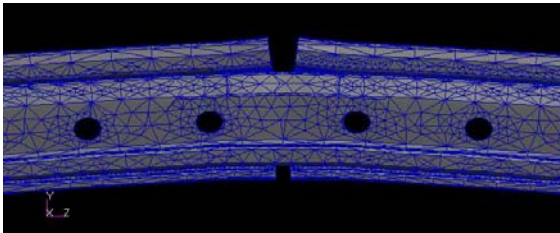


FIGURE 5.b: 0.5 Inch Debonding

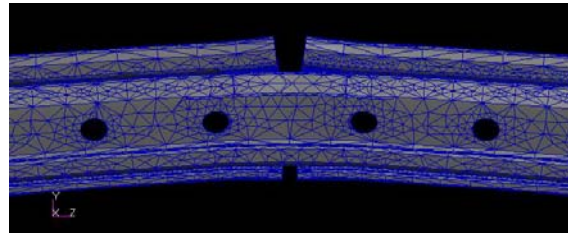


FIGURE 5.c: 1.25 Inch Debonding

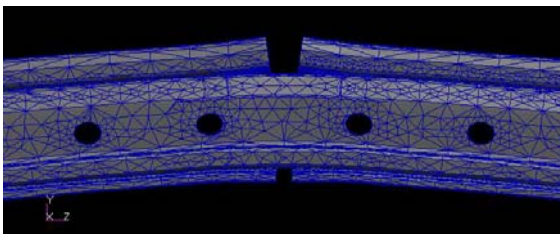


FIGURE 5.d: 2.5 Inch Debonding

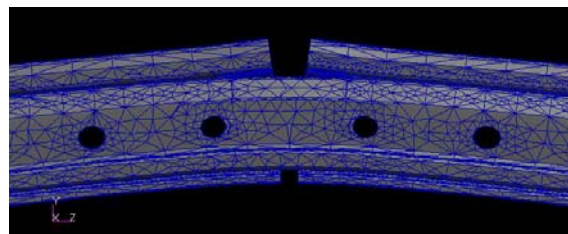


FIGURE 5.e: 3.5 Inch Debonding

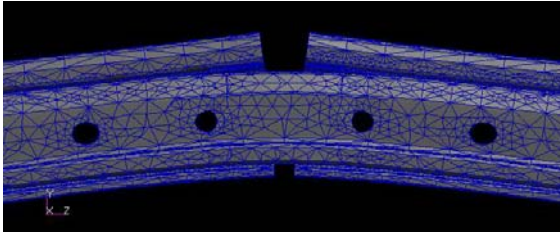


FIGURE 5.f: 8.5 Inch Debonding

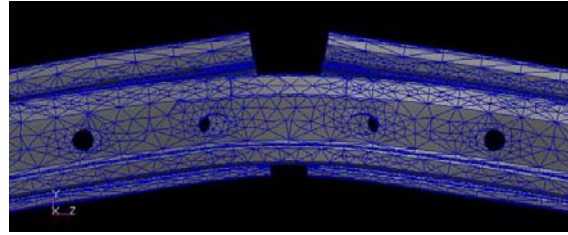


FIGURE 5: Deformation under 40k Tension (1000x Magnification)

4.2 Laterally Asymmetric Debonding

Laboratory testing of IJ strains under tension loads shows that some distressed joints develop unequal strains in the two joint bars. Figure 6 shows how this effect would occur when the epoxy debonding is more extensive on one joint bar than on the other. Partly, this is because of differences in the local stress concentrations of the two joint bars. However, the effect is amplified by out-of-plane bending forces that develop, as shown in Figure 7. In this case, the debonding *is* symmetric about the endpost, extending 3.5 inches (90 mm) in each direction under one joint bar and 2.5 inches (65 mm) in each direction under the other joint bar. Note that, at the center of the joint, the side with less debonding experiences smaller strains, while the side with more debonding experiences larger strains. Again, the effects are relatively local; the uneven strains on the two sides occur only near the debonded area.

FIGURE 6.a: 2.5 Inch Debonding

FIGURE 6.b: 3.5 Inch Debonding

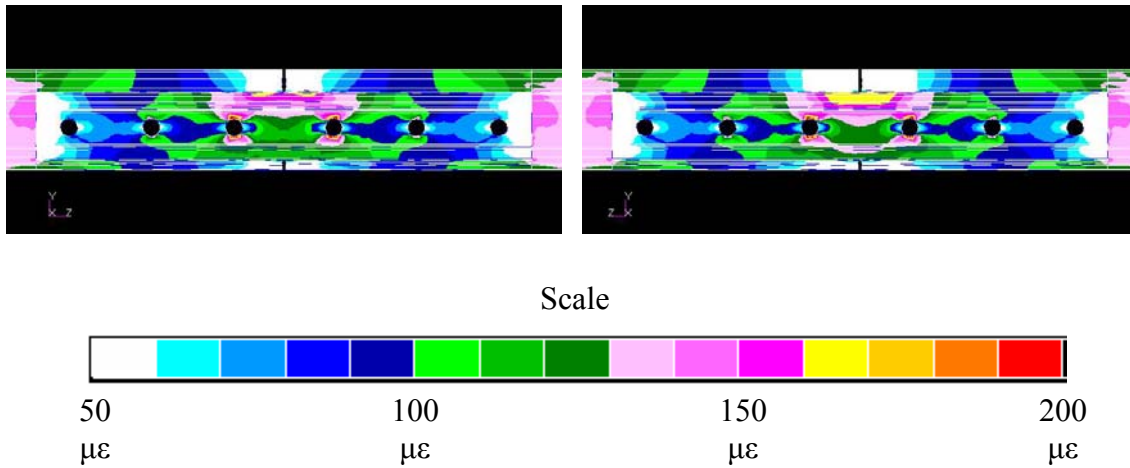


FIGURE 6: Strain In Two Sides of a Single Joint with Uneven Debonding

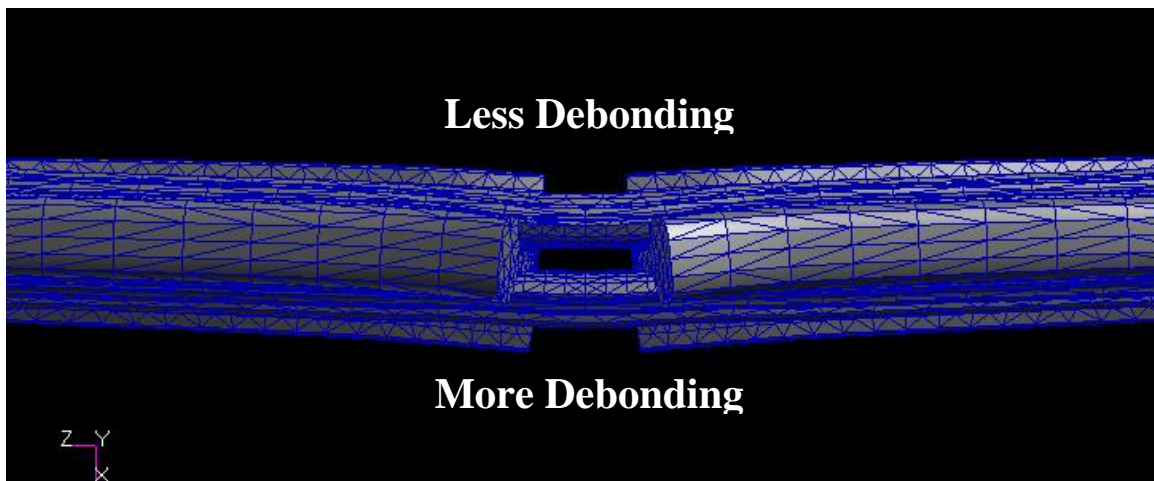


FIGURE 7: Deformation with Asymmetric Debonding (3000x Magnification)

4.3 Friction and Bolt Shear

In cases where most of the epoxy bond is still intact, shearing action in the bolts and friction at the debonded surfaces has little effect. On the other hand, when the epoxy debonding becomes extensive enough, the relative displacement between bars and rails

grows larger. This allows the bars and rails to bear directly on the bolts, concentrating forces at the edges of the bolt holes. It also creates shear stress on the debonded surfaces that exceeds the maximum static friction stress and causes slippage.

The most appropriate context for studying the effects of friction and bolt shear on an IJ is with a joint that has experienced a pull-apart. In this case, the epoxy has debonded and / or lost its structural integrity all along the length of the joint, allowing large amounts of slippage under heavy tensile loads. In this case, shear in the bolts and friction in the epoxy layer are responsible for all of the load transfer from rail to joint bar. The amount of load taken by each mechanism depends on the coefficient of static friction μ . For high values of μ , much of the load will still be transferred through the epoxy layer, and deformations will remain small. On the other hand, for $\mu = 0$, the entire load is carried by the bolts, and deformations are large. For intermediate values of μ , the frictional resistance at each location along the interface will increase as the load is applied, but only up to a point. After that, the surfaces will slide, and the bolts will take up the additional load. Note that not every point on the surface will begin slipping at the same applied load.

Figure 8 shows the strains that develop in an IJ that has pulled apart for the no-friction case ($\mu = 0$) and an intermediate case ($\mu = 0.05$). In both cases, strain at the center of the joint bar is similar to that shown in Figure 4.e and 4.f, which showed results for extensive, but not complete, debonding. Strain at the center of the joint bar for a given load seems to follow the same progression noted earlier: it increases to a maximum value as the epoxy bond begins to deteriorate, then stabilizes, and doesn't increase much more even if the joint has pulled apart.

A pull-apart occurs when debonding becomes so extensive that the shear stresses in the still-bonded epoxy regions become too high. At this point the remaining “good” areas of the epoxy layer either debond or rupture. But debonding, which results in a smooth interface, may not produce the same frictional behavior as rupture, which can produce a rough interface – for instance, between the epoxy and the fiber mesh insulator. See Figure 2 for visual examples of the difference in the interfaces produced by debonding and rupture.

Figure 9 shows one possible outcome. In this case, a value of $\mu_1 = 0.05$ was used between the endpost and the outermost bolt hole, representing the area that debonded before the pull apart; and $\mu_2 = 0.2$ was used outside of the outermost bolt hole, representing an area where the epoxy layer ruptured under heavy tensile loads. Note that with this high value of μ near the ends of the joint bar, the strain distribution takes on a pattern very similar to Figure 3.f, which had an intact epoxy bound in the same area.

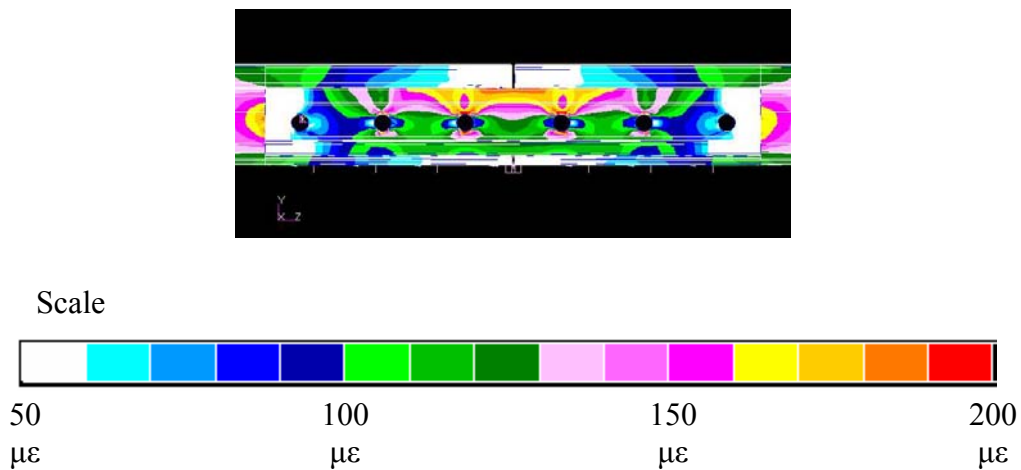


FIGURE 9: A Pulled-Apart Joint with $\mu_1 = 0.05$ and $\mu_2 = 0.2$.

5. CONCLUSIONS

The analysis results show that strain in a bonded IJ in response to longitudinal tensile loads changes as the epoxy layer comes debonded from the metal surfaces. Thus debonding can be detected and perhaps quantified using sensors placed at certain locations on the joint assembly. Strain gauges at the center of the joint bars and extensometers measuring the gap between the rail ends will show increased strain under relatively little debonding, providing an early warning of IJ deterioration. Other locations on the joint bar surface will be sensitive to different amounts of debonding. Sensors on both joint bars may be necessary in order to detect debonding reliably, as uneven debonding can lead to higher strains on one joint bar than on the other.

The load / strain relationship near the end of the joint bar after a joint has pulled apart depends very much on the frictional behavior at the epoxy / rail interface. If the pull-apart results in a higher value of μ near the ends of the joint bars, the strain from an applied tensile load will remain high. If μ is consistent along the surface, or the total friction is insufficient to carry a large percentage of the load, the strain in response to that load will be lower.

These results suggest that it is possible to monitor epoxy debonding over time by applying strain gauges and extensometers to a fully bonded joint and watching for changes in strain response. If sufficient field data can be obtained and appropriate correlations determined, this approach has the potential to provide better information about IJ condition with less lag time than current inspection practice. This improved information can in turn allow for IJ replacement to be better integrated into a well-

planned maintenance schedule, reducing the disruption caused to both maintenance and operating forces by IJ deterioration.

ACKNOWLEDGEMENTS

This project is sponsored by a grant from the Association of American Railroads under the Strategic Research Initiative and Technology Scanning programs. The first author was supported partly by a CN Railroad Engineering Fellowship. David Davis and Muhammad Akhtar of Transportation Technology Center, Inc. provided assistance and technical guidance.

Additional material and technical assistance was provided by Norfolk Southern Corporation; Portec Rail; Allegheny Rail Products (a division of L. B. Foster Co.); BNSF Railway; and CN.

REFERENCES

- (1) Cox, Joel E. *Rail Joint Mechanics*. Master's Thesis, Department of Civil Engineering, University of Delaware, 1993.
- (2) Davis, D. D.; Akhtar, M.; Kohake, E.; and Horizny, K. Effects of heavy axle loads on bonded insulated joint performance, *Proceedings of the AREMA 2005 Annual Conference*, Chicago, IL, 2005.
- (3) *United States Code of Federal Regulations*, Title 49, Part 213.119.g, 10/1/06 ed. Accessed at http://edocket.access.gpo.gov/cfr_2006/octqtr/pdf/49cfr213.119.pdf on 7/30/2007.

- (4) American Railway Engineering Association. *Stresses in Railroad Tracks – The Talbot Reports*, published by the AREA, Washington DC, 1980.
- (5) Jenkins, H. H.; Stephenson, J. E.; Clayton, G. A.; Morland, G. W.; and Lyon, D. “The effect of track and vehicle parameters on wheel / rail vertical dynamic forces”, *Railway Engineering Journal*, v3, n1, Jan, 1974, p 2-16.
- (6) Suzuki, T.; Ishida, M.; Kazuhisa, A.; and Kazuhiro, K. “Measurement on dynamic behaviour of track near rail joints and prediction of track settlement,” *Quarterly Report of RTRI (Railway Technical Research Institute) (Japan)*, v 46, n 2, 2005, p 124-129.
- (7) Kerr, Arnold D. and Cox, Joel E. “Analysis and tests of bonded insulated rail joints subjected to vertical wheel loads,” *International Journal of Mechanical Sciences*, v41, n 10, Oct, 1999, p. 1253-1272.
- (8) Li, D.; Meddah, A.; Davis, D.; and Kohake, E. “Performance of insulated joints at western mega site,” Transportation Technology Center, Inc. Technology Digest TD-06-28, December 2006.
- (9) Akhtar, Muhammad N. and Davis, David D. “Preliminary results of prototype insulated joint tests at FAST,” Transportation Technology Center, Inc. Technology Digest TD-07-13, May 2007.
- (10) Himebaugh, Anne K. *Finite Element Analysis of Insulated Rail Joints*. Master’s Thesis, Department of Civil Engineering, Virginia Polytechnic Institute and State University, 2006.
- (11) *2000 Manual for Railway Engineering*, The American Railway Engineering and Maintenance of Way Association, 2000, Chapter 4.